

O_2-Binding Properties of Double-Sided Porphinatoiron(II)s with Polar Substituents and Their Human Serum Albumin Hybrids

Teruyuki Komatsu, Tomoyuki Okada, Miho Moritake, and Eishun Tsuchida[*,#]

Department of Polymer Chemistry, Advanced Research Institute for Science and Engineering, Waseda University, Tokyo 169-8555

(Received February 15, 2001)

Double-sided porphinatoiron(II)s with polar substituents [R; hydroxy (**FeDP(OH)**), methoxy (**FeDP(OMe)**), and acetoxy (**FeDP(OAc)**)] on the 2,2-dimethylpropanoyloxy-fence groups have been synthesized. **FeDP(OMe)** and **FeDP(OAc)** formed five-*N*-coordinated high-spin Fe^{2+} complexes with an intramolecularly bound axial imidazole in toluene (or CH_2Cl_2) under an N_2 atmosphere. Upon the addition of O_2, they produced stable O_2 adducts at 25 °C; their half-lives in water-saturated toluene (50–77 h) are 2–3 fold longer compared to that of the single-face encumbered porphinatoiron(II) (**FeP**). Their O_2-binding parameters are almost identical to that of **FeDP(H)**, which has nonpolar substituents on the fences. In contrast, **FeDP(OH)** showed a significantly low O_2-binding affinity and was immediately oxidized to the Fe^{3+} state after contact with bubbling O_2 gas. The incorporation of these FeDPs into the human serum albumin (HSA) provided artificial hemoproteins, which can reversibly bind and release O_2 under physiological conditions (in aqueous media, pH 7.3, 37 °C) like hemoglobin and myoglobin. The half-life of the dioxygenated HSA–**FeDP(H)** reached 5 h (37 °C). This corresponded to a 2.5-fold increase compared to that of HSA–**FeP**. The time dependences of the absorption changes accompanying the O_2- and CO-rebindings to the HSA–FeDPs after laser flash photolysis were composed of two phases. These observations indicate that the recombination of O_2 and CO to the central Fe^{2+} ion is affected by the microenvironments around the FeDPs in the HSA structure, e.g. a steric hindrance of the amino acid residue and a difference in polarity. Furthermore, **FeDP(H)** incorporated into HSA showed a high stability against H_2O_2.

A simple, but serious, problem often found in synthetic hemoprotein models is the short lifetimes of their biological activities under physiological conditions, namely in water (pH 7.3) at 37 °C. In order to alleviate this fault, both-faces encumbered porphinatoirons have been synthesized to inhibit unfavorable side-reactions by a steric hindrance on both sides of the porphine ring.[1–5] We have also found that 5,10,15-tris[2,6-bis(2,2-dimethylpropanoyloxy)phenyl]-20-{2-(2,2-dimethylpropanoyloxy)-6-[5-(1-imidazolyl)pentanoyloxy]phenyl}porphinatoiron(II) [double-sided porphinatoiron(II) (**FeDP(H)**)] formed a stable O_2-adduct with a lifetime on the order of one day in not only toluene solution, but also aqueous media, by embedding into the bilayer membrane of phospholipid vesicles (Chart 1).[6]

On the other hand, it has been shown that human serum albumin (HSA) incorporating 5,10,15,20-tetrakis[$\alpha,\alpha,\alpha,\alpha$-*o*-(2,2-dimethylpropanamido)phenyl]-2-[8-(2-methyl-1-imidazolyl)octanoyloxymethyl]porphinatoiron(II) (**FeP**) (HSA–**FeP**) can reversibly bind and release O_2 under physiological conditions, like Hb and Mb.[7] Since the serum albumin is the abundant plasma protein, the biological advantage is significant compared to the phospholipid vesicles as a vehicle for porphinatoirons. The obtained HSA–FeP solution has good compatibility with human whole blood and can quantitatively transport O_2 in vivo.[7b,c,8] At present, HSA–**FeP** has become one of the most promising materials as *a red cell substitute*.

On the basis of these two findings, we expect that the combination of the double-sided porphinatoirons (FeDPs) and HSA can provide a novel O_2-carrying hemoprotein, which can form a more stable O_2-adduct complex. Recently, new double-sided porphinatoiron(II)s with different polar substituents on the 2,2-dimethylpropanoyloxy-fence groups have been synthesized to increase the compatibility of porphyrin to HSA, and control the O_2-binding equilibrium. A polar substituent around the O_2-binding site of the synthetic heme generally increases its O_2-binding affinity, which is due to a decrease in the O_2-dissociation rate constant (*polarity effect*).[9–11] This kind of work was mostly done in the 1980's, but has recently gained attention again for analogues to the site-directed mutagenesis of the distal residues in O_2-binding hemoproteins.[12,13] This paper describes the O_2-binding equilibria and kinetics of the newly synthesized double-sided porphinatoiron(II)s with different polar substituents in organic solvents. The O_2-binding properties of the HSA hybrids incorporating these FeDPs in aqueous media are also evaluated in detail. Furthermore, we have found that **FeDP(H)** incorporated into HSA shows high stability against H_2O_2.

Experimental

Materials and Apparatus. Infrared spectra were recorded with a JASCO FT/IR-410 spectrometer. ^{1}H NMR spectra were measured using a JEOL Lambda 500 spectrometer. Chemical shifts were expressed in parts per million downfield from Me_4Si as an internal standard. FAB-MS spectra were obtained from a

CREST investigator, JST.

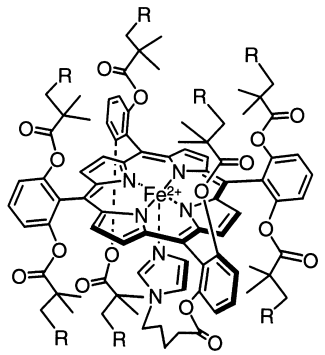

R: —H **FeDP(H)**
—OH **FeDP(OH)**
—O— **FeDP(OMe)**
—O—C(=O)— **FeDP(OAc)**

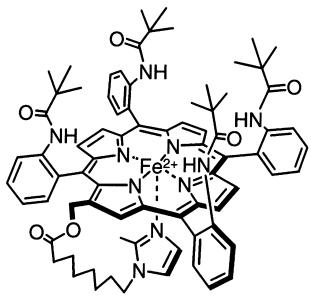

FeP

Chart 1.

JEOL JMS-SX102A spectrometer. UV-vis absorption spectra were recorded on a JASCO V-570 spectrophotometer. Thin-layer chromatography (TLC) was carried out on 0.2 mm precoated plates of silica-gel 60 F_{254} (Merck). Purification was performed by a silica-gel 60 (Merck) column or flash-column chromatography. 5,10,15,20-Tetrakis(2,6-dihydroxyphenyl)porphine, and 5-(1-imidazolyl)pentanoic acid were prepared according to previously reported procedures.[6] All solvents were purified by distillation before use. Other chemicals were of commercial high-purity grades and not further purified. The water used was deionized using an ADVANTEC GS-200 system. An HSA was purchased from Bayer Co., Ltd. (Albumin Cutter, 5 wt%). Isoelectric points were measured by a Pharmacia Phastsystem using isoelectric focusing (IEF) in pH 3–9 Phast Gel IEF 3–9.[7b] The temperature during the electrophoresis was maintained at 15 °C. The markers used were from an Isoelectric Focusing Calibration Kit.

3-Methoxy-2,2-dimethylpropanoic Acid (3). Sodium hydride (60%) (6.0 g, 149.8 mmol) was dispersed to a dry THF solution (500 mL) of methyl 3-hydroxy-2,2-dimethylpropanoate (**1**) (19.8 g, 149.8 mmol), and stirred for 2 h at 0 °C and 2 h at room temperature. Iodomethane (14 mL, 224.7 mmol) was then added dropwise to the mixture. After stirring for 12 h, the solvent was brought to dryness on a rotary evaporator and $CHCl_3$ extracted the residue. The organic layer was washed with water several times and dried over anhydrous Na_2SO_4. The vacuum distillation of this mixture under 1.6 kPa at 43 °C yielded methyl 3-methoxy-2,2-dimethylpropanoate (**2**) as a transparent liquid (6.83 g, 31%). R_f = 0.78 ($CHCl_3$). IR (NaCl) 1111 (COC (ether)), 1736 (C=O (ester)) cm^{-1}. ^1H NMR ($CDCl_3$) δ 1.1 (6H, s, –$C(CH_3)_2$–), 3.2 (3H, s, CH_3OCH_2–), 3.3 (2H, s, CH_3OCH_2–), 3.6 (3H, s, –CO(=O)CH_3).

Five% ethanolic KOH (34.0 mL) was added to a THF solution (5 mL) of **2** (3.0 g, 20.5 mol) and stirred for 12 h at 45 °C. After the solvent was evaporated, the residue was dissolved again to $CHCl_3$ and carefully neutralized by hydrochloric acid. The organic layer was washed with water and dried in vacuo to give 3-methoxy-2,2- dimethylpropanoic acid (**3**) as transparent liquid (1.06 g, 62%). IR (NaCl) 1122 (COC (ether)), 1704 (C=O), 3100 (OH) cm^{-1}. ^1H NMR ($CDCl_3$) δ 1.2 (6H, s, –$C(CH_3)_2$–), 3.3 (3H, s, CH_3OCH_2–), 3.4 (2H, s, CH_3OCH_2–).

5-[6-Hydroxy-2-(3-methoxy-2,2-dimethylpropanoyloxy)-phenyl]-10,15,20-tris[2,6-bis(3-methoxy-2,2-dimethylpropanoyloxy)phenyl]porphine (4). Thionyl chloride (0.72 mL, 9.82 mmol) was added to **3** (259 mg, 1.96 mmol) under an argon atmosphere and stirred for 1 h at room temperature. Excess of thionyl chloride was removed in vacuo (5.3 kPa) and dissolved in dry THF (30 mL). This solution was then added dropwise to a THF solution of 5,10,15,20-tetrakis(2,6-dihydroxyphenyl)porphine (200 mg, 0.269 mmol) and 4-(dimethylamino)pyridine (230 mg, 1.88 mmol) at room temperature, and refluxed for 12 h. The obtained mixture was brought to dryness on a rotary evaporator and extracted with $CHCl_3$. The organic layer was then washed with water and the evaporated residue was chromatographed on silica-gel flash-column using $CHCl_3/CH_3OH$ (15/1 v/v) as the eluent. The second band eluted was collected and reduced to a small volume on a rotary evaporator. The residue was dried at room temperature for several hours in vacuo to give compound **4** as purple crystals (42.4 mg, 10%). R_f = 0.44 ($CHCl_3/CH_3OH$, 15/1 v/v). IR (NaCl) 1098 (COC (ether)), 1756 (C=O(ester)), 3454 (OH) cm^{-1}. UV-vis ($CHCl_3$) λ_{max} (10^{-3} ε (M^{-1} cm^{-1})) 417 (410), 510 (25), 541 (4.0), 586 (7.8), 638 nm (0.93). ^1H NMR ($CDCl_3$) δ −3.0 (2H, d, innerH), −0.7–−0.2 (42H, m, –$C(CH_3)_2$–), 0.9–2.4 (21H, m, CH_3O–), 2.5–2.7 (14H, m, CH_3OCH_2–), 6.9–7.9 (12H, m, Phenyl), 8.8 (8H, d, pyrrole-β). FAB-MS: *m/z* 1541.2 [M^+].

5-{6-[5-(1-Imidazolyl)pentanoyloxy]-2-(3-methoxy-2,2-dimethylpropanoyloxy)phenyl}-10,15,20-tris[2,6-bis(3-methoxy-2,2-dimethylpropanoyloxy)phenyl]porphine (5). After oxalyl chloride (1.0 mL, 11.5 mmol) was added to a dry CH_3CN (20 mL) solution of 5-(1-imidazolyl)pentanoic acid hydrochloride[5] (87.8 mg, 0.429 mmol) under an argon atmosphere, the mixture was stirred for 1 h at 65 °C. The excesses of oxalyl chloride and CH_3CN were removed in vacuo to yield a pale-yellow solid. A dry CH_3CN (10 mL) solution of **4** (42.4 mg, 0.0286 mmol) and 4-(dimethylamino)pyridine (78.6 mg, 0.643 mmol) was added dropwise to this acid chloride at room temperature under an argon atmosphere and darkness. The solution was then refluxed for a further 12 h. After the solvent was evaporated, $CHCl_3$ extracted the residue, which was dried over anhydrous Na_2SO_4. The obtained mixture was chromatographed on a silica-gel flash-column using $CHCl_3/CH_3OH$ (8/1 v/v) as the eluent. The major band was collected and dried at room temperature for several hours in vacuo to give compound **5** as purple crystals (35.4 mg, 74%). R_f = 0.50 ($CHCl_3/CH_3OH$, 8/1 v/v). IR (NaCl) 1102 (COC (ether)), 1760 (C=O (ester)) cm^{-1}. UV-vis ($CHCl_3$) λ_{max} (10^{-3} ε (M^{-1} cm^{-1})) 416 (420), 510 (26), 541 (4.1), 586 (8.0), 640 nm (0.96). ^1H NMR ($CDCl_3$) δ −3.0 (2H, s, innerH), −0.6–−0.2 (42H, m, –$C(CH_3)_2$–), 0.8–2.2 (20H, m, $ImCH_2(CH_2)_3$–, CH_3OCH_2–), 3.6–3.7 (2H, m, $ImCH_2$–), 6.6, 6.9, 7.2 (3H, 3s, Im), 7.4–7.9 (12H, m, phenyl), 8.8 (8H, m, pyrrole-β). FAB-MS: *m/z* 1691.7 [M^+].

Fe^{3+}DP(OMe) Cl^-. $Fe(CO)_5$ (0.082 mL, 630 μmol) and I_2

(5.3 mg, 21 μmol) were added to a dry toluene solution (4.0 mL) of **5** (17.7 mg, 10.5 μmol) under an argon atmosphere. After the mixture was heated at 110 °C for 3 h, an aqueous NaCl solution was added at room temperature. $CHCl_3$ extracted the dispersion, which was washed with water. After drying over anhydrous Na_2SO_4, the organic layer was evaporated to dryness and the residue was chromatographed on a silica-gel flash-column using $CHCl_3/CH_3OH$ (10/1 v/v) as eluent. The major band was collected and dried at room temperature for several hours in vacuo to give $Fe^{3+}DP(OMe)\ Cl^-$ as purple crystals (14.6 mg, 78%). R_f = 0.44 ($CHCl_3/CH_3OH$, 10/1 v/v). IR (NaCl) 1098 (COC (ether)), 1760 (C=O (ester)) cm^{-1}. UV-vis ($CHCl_3$) λ_{max} ($10^{-4}\ \varepsilon$ ($M^{-1}\ cm^{-1}$)) 341 (3.9), 416 (12), 508 (1.2), 575 nm (0.81). FAB-MS: *m/z* 1745.2 [M^+-Cl]. Found: C, 64.78; H, 6.55; N, 4.23%. Calcd for $C_{94}H_{108}N_6O_{23}FeCl\cdot C_6H_6$: C, 64.60; H, 6.28; N, 4.52%

3-Benzyloxy-2,2-dimethylpropanoic Acid (7). This compound was prepared according to a similar manner of **3**, except for using benzyl bromide. From the crude material, methyl 3-benzyloxy-2,2-dimethylpropanoate (**6**) was purified by removing the unreacted benzyl bromide and **1** under 1.7 kPa at 75 °C (5.65 g, 68%). After saponification, 3-benzyloxy-2,2-dimethylpropanoic acid (**7**) was given as white crystals (921 mg, 38%). R_f = 0.54 ($CHCl_3$/MeOH, 30/1 v/v). IR (NaCl) 1100 (COC (ether)), 1704 (C=O), 2900 (OH) cm^{-1}. ^{1}HNMR ($CDCl_3$) δ 1.2 (6H, s, $-C(CH_3)_2-$), 3.5 (2H, s, BzlOCH_2–), 4.6 (2H, s, PhCH_2–), 7.3–7.4 (5H, m, phenyl).

5-[2-(3-Benzyloxy-2,2-dimethylpropanoyloxy)-6-hydroxyphenyl]-10,15,20-tris-[2,6-bis(3-benzyloxy-2,2-dimethylpropanoyloxy)phenyl]phenylporphine (8). Oxalyl chloride (1.23 mL, 14.1 mmol) was added to **7** (589 mg, 2.83 mmol) under an argon atmosphere and stirred for 1.5 h at room temperature. Excess of oxalyl chloride was removed in vacuo, and the residue was dissolved in dry THF (30 mL). The obtained solution was slowly added dropwise to a THF solution (100 mL) of 5,10,15,20-tetrakis(2,6-dihydroxyphenyl)porphine (300 mg, 0.404 mmol) and 4-(dimethylamino)pyridine (346 mg, 2.83 mmol) at room temperature, and the mixture was refluxed for 3 h. After the evaporation of THF, $CHCl_3$ extracted the mixture. The organic layer was washed with water and dried over anhydrous Na_2SO_4. The solvent was then removed and the residue was chromatographed on a silica-gel flash-column using $CHCl_3/CH_3OH$ (40/1 v/v) as the eluent. The second band eluted was collected and dried at room temperature for several hours in vacuo to give compound **8** as purple crystals (104 mg, 13%). R_f = 0.34 ($CHCl_3/CH_3OH$, 40/1 v/v). IR (NaCl) 1100 (COC (ether)), 1759 (C=O (ester)), 3450 (OH (alcohol)) cm^{-1}. UV-vis ($CHCl_3$) λ_{max} ($10^{-3}\ \varepsilon$ ($M^{-1}\ cm^{-1}$)) 416 (400), 510 (27), 541 (4.0), 585 (8.4), 638 nm (0.93). ^{1}H NMR ($CDCl_3$) δ −3.0 (2H, d, innerH), −0.9–−0.5 (42H, m, $-C(CH_3)_2-$), 2.1–2.8 (14H, m, BzlOCH_2–), 3.8–4.3 (14H, m, PhCH_2–), 6.8–7.8 (47H, m, phenyl), 8.8 (8H, d, pyrrole-β) . FAB-MS *m/z* 2073.5 [M^+-H].

5-{2-(3-Benzyloxy-2,2-dimethylpropanoyloxy)-6-[5-(1-imidazolyl)pentanoyloxy]phenyl}-10,15,20-tris[2,6-bis(3-benzyloxy-2,2-dimethylpropanoyloxy)phenyl]porphine (9). The introduction of the (1-imidazolyl)alkyl arm to **8** was carried out according to the same procedure for **5**, as described above. The compound **9** was afforded as purple crystals (64.8 mg, 60%). R_f = 0.27 ($CHCl_3/CH_3OH$, 20/1 v/v). IR (NaCl) 1097 (COC (ether)), 1760 (C=O (ester)) cm^{-1}. UV-vis ($CHCl_3$) λ_{max} ($10^{-3}\ \varepsilon$ ($M^{-1}\ cm^{-1}$)) 416 (430), 509 (27), 539 (4.2), 584 (8.2), 639 nm (1.0). ^{1}H NMR ($CDCl_3$) δ −3.1 (2H, s, innerH), −1.1–−0.5 (42H, m, $-C(CH_3)_2-$), 0.8–0.9 (4H, m, $ImCH_2(CH_2)_2-$), 1.2 (2H, m, $ImCH_2-$), 2.4–2.8 (14H, m, BzlOCH_2–), 3.4 (4H, m, $Im(CH_2)_3CH_2-$), 3.9–4.3 (14H, m, $PhCH_2-$), 6.6, 6.9 (2H, 2s, Im), 7.1–7.8 (47H, m, Phenyl, Im), 8.8 (8H, m, pyrrole-β). FAB-MS: *m/z* 2224.2 [M^+].

5-{2-(3-Hydroxy-2,2-dimethylpropanoyloxy)-6-[5-(1-imidazolyl)pentanoyloxy]phenyl}-10,15,20-tris[2,6-bis(3-hydroxy-2,2-dimethylpropanoyloxy)phenyl]porphine (10). Boron trifluoride diethyl ether complex (332 μL, 2.63 mmol) and ethanethiol (1.36 mL, 18.4 mmol) were added to the CH_2Cl_2 solution of **9** (16.2 mg, 7.28 μmol). After stirring for 2.5 h at room temperature, water was added to stop the reaction and $CHCl_3$ extracted the mixture. The organic layer was washed with water and dried over anhydrous Na_2SO_4. The residue was chromatographed on a silica-gel flash-column using $CHCl_3/CH_3OH$ (6/1 v/v) as the eluent. The major band was collected and dried at room temperature for several hours in vacuo to give compound **10** as purple crystals (13.6 mg, 44%). R_f = 0.40 ($CHCl_3/CH_3OH$, 6/1 v/v). IR (NaCl) 1756 (C=O (ester)), 3435 (OH (alcohol)) cm^{-1}. UV-vis ($CHCl_3$) λ_{max} ($10^{-3}\ \varepsilon$ ($M^{-1}\ cm^{-1}$)) 417 (390), 512 (23), 546 (3.8), 582 (8.6), 634 nm (0.92). ^{1}H NMR ($CDCl_3$) δ −3.3 (2H, s, innerH), −0.1–0.4 (42H, m, $-C(CH_3)_2-$), 0.8–0.9 (4H, m, $ImCH_2(CH_2)_2-$), 1.0–1.5 (16H, m, $HOCH_2-$, $Im(CH_2)_3CH_2-$), 3.6 (2H, m, $ImCH_2-$), 6.6, 6.8, 7.2 (3H, 3s, Im), 7.4–7.9 (12H, m, phenyl), 8.8 (8H, m, pyrrole-β). FAB-MS: *m/z* 1593.2 [M^+].

$Fe^{3+}DP(OH)Cl^-$. Iron insertion to the compound **10** was performed by the same procedure as described above. $Fe^{3+}DP(OH)\ Cl^-$ was obtained as a purple crystalline (12.9 mg, 95%). R_f = 0.32 ($CHCl_3/CH_3OH$, 6/1 v/v). IR (NaCl) 1753 (C=O (ester)), 3372 (OH) cm^{-1}. UV-vis ($CHCl_3$): λ_{max} ($10^{-4}\ \varepsilon$ ($M^{-1}\ cm^{-1}$)) 342 (2.5), 418 (9.0), 509 (0.74), 586 nm (0.42). FAB-MS: *m/z* 1647.4 [M^+-Cl]. Found: C, 61.69; H, 5.31; N, 4.32%. Calcd for $C_{87}H_{94}N_6O_{23}FeCl\cdot H_2O$: C, 61.98; H, 5.64; N, 4.05%

5-{2-(3-Acetoxy-2,2-dimethylpropanoyloxy)-6-[5-(1-imidazolyl)pentanoyloxy]phenyl}-10,15,20-tris[2,6-bis(3-acetoxy-2,2-dimethylpropanoyloxy)phenyl]porphine (11). Acetyl chrolide (0.186 mL, 2.64 mmol) was added to a dry THF solution (8 mL) of **10** (20 mg, 0.0126 mmol) and pyridine (0.268 mL, 2.64 mmol). The mixture was stirred for 2 h at room temperature and brought to dryness on a rotary evaporator. The residue was extracted with $CHCl_3$ and the organic layer was washed with water. After drying over anhydrous Na_2SO_4, the organic layer was evaporated and chromatographed on a silica-gel flash-column using $CHCl_3/CH_3OH$ (6/1 v/v) as the eluent. The major band was collected and dried at room temperature for several hours in vacuo to give compound **11** as purple crystals (13.3 mg, 65%). R_f = 0.57 ($CHCl_3/CH_3OH$, 6/1 v/v). IR (NaCl) 1738, 1759 (C=O (ester)) cm^{-1}. UV-vis ($CHCl_3$) λ_{max} ($10^{-3}\ \varepsilon$ ($M^{-1}\ cm^{-1}$)) = 416 (430), 510 (27), 541 (4.9), 586 (8.6), 638 nm (1.1). ^{1}H NMR ($CDCl_3$) δ −3.1 (2H, s, innerH), −0.9–−0.4 (42H, m, $-C(CH_3)_2-$), 0.9 (4H, m, $ImCH_2(CH_2)_2-$), 1.3–1.8 (23H, m, $CH_3C(=O)O-$, $Im(CH_2)_3CH_2-$), 3.0–3.4 (14H, m, AcOCH_2–), 3.7 (2H, m, $ImCH_2-$) 6.7, 6.9, 7.2 (3H, 3s, Im), 7.3–7.9 (12H, m, phenyl), 8.8 (8H, m, pyrrole-β). FAB-MS: *m/z* 1887.0 [M^+-H].

$Fe^{3+}DP(OAc)\ Cl^-$. Iron insertion to compound **10** was carried out using the same procedure as that for $Fe^{3+}DP(OMe)Cl^-$, as described above. $Fe^{3+}DP(OAc)\ Cl^-$ was obtained as purple crystal (12.9 mg, 94%). R_f = 0.59 ($CHCl_3/CH_3OH$ = 6/1 (v/v)). IR (NaCl) 1737, 1759 (C=O (ester)) cm^{-1}. UV-vis ($CHCl_3$) λ_{max} ($10^{-4}\ \varepsilon$ ($M^{-1}\ cm^{-1}$)) = 341 (3.4), 416 (11), 507 (1.1), 578 nm (0.71). FAB-MS: *m/z* 1941.3 [M^+-Cl]. Found: C, 62.22; H, 5.66; N, 4.38%. Calcd for $C_{101}H_{108}N_6O_{30}FeCl\cdot C_6H_6$: C, 62.53; H, 5.59; N, 4.09%

Reduction of Fe^{3+} Complex to Fe^{2+} Complex in Organic Solvent. Reduction to the porphinatoiron(II) complex was carried out using toluene (or CH_2Cl_2) − aq $Na_2S_2O_4$ in a heterogeneous two-phase system under aerobic conditions, as previously reported.[6,14] After separation of the two phases, the organic layer containing the reduced compound was transferred into a cuvette under an Ar atmosphre. A Karl Fisher's reagent (Kyoto Electronic Ind.) measured the water content in the obtained organic solution. The concentration of the water in a toluene solution was 0.048 wt% and 0.22 wt% in CH_2Cl_2, which shows the good agreement with the literature values.

Preparation of HSA–FeDP Hybrid. The HSA–FeDP hybrid was prepared by the following procedure. Aqueous ascorbic acid (17 mM, 37 μL) was added to a DMSO solution of an Fe(III)DP derivative (133 μM, 5 mL) under carbon monoxide (CO). Partial reduction of the central Fe^{3+} ion occurred in this stage. Then, the obtained solution was photoirradiated with a 250-W ultra high-pressure Hg arc-lamp (Ushio UCH-250).[15] After complete reduction, the UV-vis absorption spectrum showed the formation of a six-coordinated carbonyl complex. This CO complex in DMSO was injected into the phosphate buffer solution (33 mM, pH 7.3) of HSA (17 μM, pH 7.3, 20 mL) under a CO atmosphere, and the mixture was dialyzed with a cellulose membrane against a phosphate buffer (pH 7.3) for 2 h and 15 h at 4 °C. At the last, the total volume was adjusted to 33 mL, giving an HSA–FeDP(CO) solution (FeDP/HSA = 8 (mol/mol), [Fe] = 20 μM).

Binding Numbers of FeDP into HSA. Based on the absorbance intensity of the UV-vis absorption spectra of the HSA–FeDP(CO) hybrid with different FeDP/HSA mixing ratios, the binding numbers of FeDP in the albumin host were assayed.[7b,c]

O_2- and CO-Coordination Equilibria and Kinetics. The O_2- and CO-bindings to FeDP derivative are expressed by

$$\mathrm{FeDP} + \mathrm{L} \underset{k_{\mathrm{off}}{}^{\mathrm{L}}}{\overset{k_{\mathrm{on}}{}^{\mathrm{L}}}{\rightleftharpoons}} \mathrm{FeDP(L)} \qquad (1)$$

$$(K = k_{\mathrm{on}}{}^{\mathrm{L}}/k_{\mathrm{off}}{}^{\mathrm{L}})$$

The O_2-binding affinity (the pressure at half O_2-binding for FeDP, $P_{1/2}{}^{\mathrm{L}} = 1/K^{\mathrm{L}}$) of FeDPs in organic solvents or their HSA hybrids in aqueous media was determined by spectral changes at various partial pressures of O_2 as in previous literature.[6,14,16,17] The FeDPs concentrations of 20 μM were normally used for UV-vis absorption spectroscopy. The spectra were recorded within the range of 350–700 nm. The O_2- and CO-association and -dissociation rate constants (k_{on}, k_{off}) were measured by a competitive rebinding technique using a Unisoku TSP-600 laser-flash photolysis apparatus.[6,14,16,17] Because of the absorption decays accompanied O_2- and CO-rebinding to FeDPs in organic solvents obeyed a single exponential, we applied a first-order kinetics to calculate the rates. On the other hand, HSA–FeDP hybrid in aqueous solution showed triphases. We employed triple-exponential kinetics to analyze the absorption decays.[7d]

Results and Discussion

O_2-Coordination Properties of FeDPs in Organic Solvents. Double-sided porphinatoiron(II)s with polar substituents [R; hydroxy (**FeDP(OH)**), methoxy (**FeDP(OMe)**), and acetoxy (**FeDP(OAc)**)] on the 2,2-dimethylpropanoyloxyfence groups have been synthesized according to the modified procedure of **FeDP(H)** using the corresponding acid chlorides (Scheme 1). The obtained Fe^{3+} compounds were converted to the Fe^{2+} complex by reduction in a heterogeneous two-phase system (toluene or CH_2Cl_2 with aq $Na_2S_2O_4$) under an N_2 atmosphere. For instance, the UV-vis absorption spectrum of the orange solution of **FeDP(OMe)** showed the formation of a five-*N*-coordinated complex ($\lambda_{\max}$: 437, 544, 560 nm, Fig. 1), which was constant in the range from 5 μM–1 mM at 10–70 °C. The paramagnetic $S = 2$ state of **FeDP(OMe)** was determined by the β-pyrrolic proton signals at 50.2, 50.5, 56.0, 57.7 ppm downfield to TMS (25 °C). No peaks between −5 and −15 ppm demonstrated that a square-planar Fe^{2+} porphinate ($S = 1$) did not exist.[18] We can conclude that **FeDP(OMe)** is a five-coordinated high-spin Fe^{2+} complex with an intramolecularly bound imidazole under an N_2 atmosphere. These results are consistent with the data of **FeDP(H)**, which has no p olar substituents on the fences.[6] **FeDP(OAc)** also showed the same results ($\lambda_{\max}$: 437, 544, 560 nm, and β-pyrrolic proton signals at

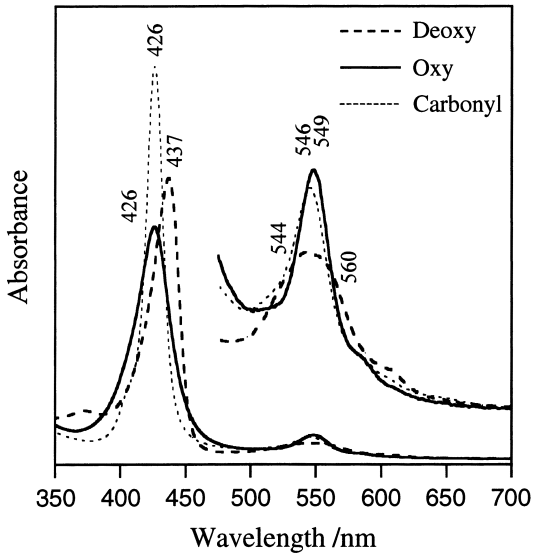

Fig. 1. Visible absorption spectral changes of **FeDP(OMe)** in toluene solution at 25 °C.

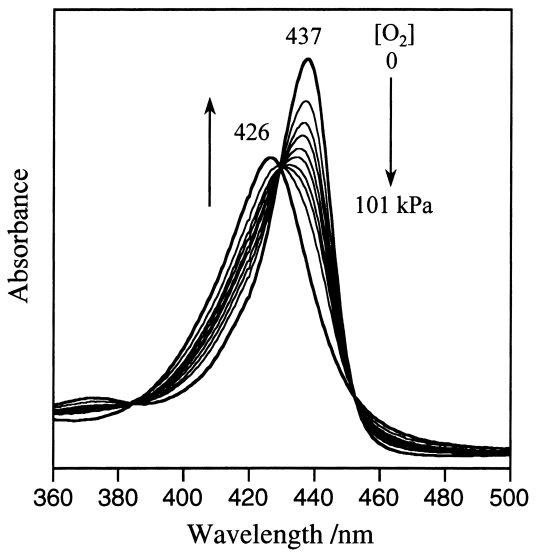

Fig. 2. Visible absorption spectral changes of **FeDP(OMe)** during the O_2-titration in toluene solution at 25 °C.

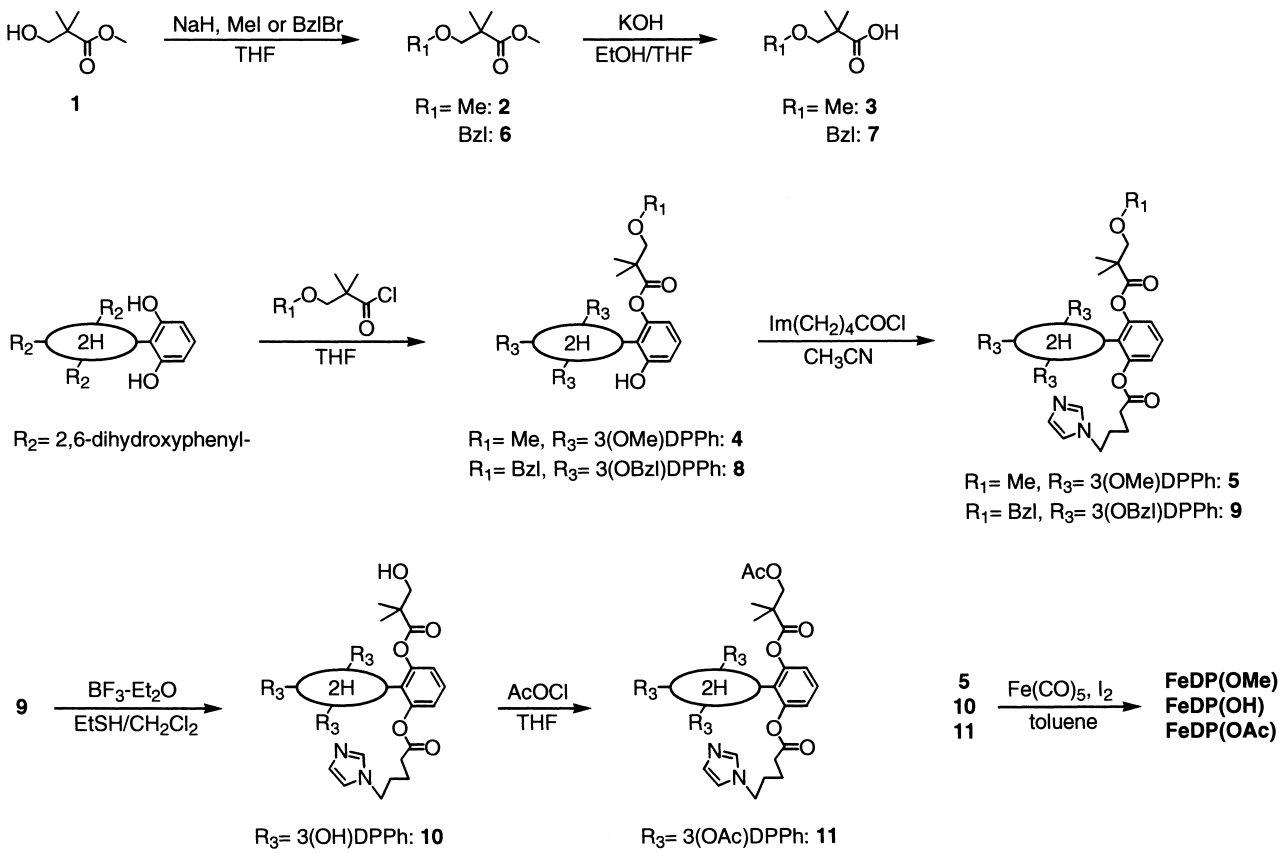

3(OMe)DPPh: 2,6-bis(3-methoxy-2,2-dimethylpropanoyloxy)phenyl-, 3(OBzl)DPPh: 2,6-bis(3-benzyloxy-2,2-dimethylpropanoyloxy)phenyl-, 3(OH)DPPh-: 2,6-bis(3-hydroxy-2,2-dimethylpropanoyloxy)phenyl-, 3(OAC)DPPh: 2,6-bis(3-acethoxy-2,2-dimethylpropanoyloxy)phenyl-

Scheme 1.

51.1, 51.2, 56.2, 58.1 ppm). In contrast, the UV-vis absorption maxima of **FeDP(OH)** appeared at different positions (426, 534, 559 nm), which may suggest partial coordination of the hydroxy group to the Fe^{2+} center.

Upon exposure of these FeDPs solutions to O_2 or CO, the UV-vis absorptions immediately changed to those of the O_2 or CO adduct complex, respectively. The dioxygenations were kinetically stable and reversible at 25 °C, depending on the O_2-partial pressure (Fig. 2); however, the oxidation to the Fe^{3+} porphinate slowly took place by a proton-driven process in water-saturated toluene, and the final products were actually all Fe^{3+}OH complexes with λ_{max} at 417 and 576 nm. The seven fences on the ring plane obviously prevent μ-oxo porphine dimer formation. The half-lives ($\tau_{1/2}$) of the O_2-addducts were determined to be 50–77 h. (25 °C, under 1 atm O_2) for **FeDP(H)**, **FeDP(OMe)**, and **FeDP(OAc)** (Table 1), which are all 2–3-fold longer compared to that of **FeP** (24 h) under the same conditions.[14]

On the other hand, the dioxygenated **FeDP(OH)** has very short lifetime ($\tau_{1/2}$: 0.2 h). It has been reported that the introduction of a flexible protic group around the O_2-binding site accelerates irreversible oxidation.[10,12] The same situation probably holds true for **FeDP(OH)**.

The O_2-binding affinities ($P_{1/2}{}^{O_2}$), and association and disso-

Table 1. O_2-Binding Parameters of Double-Sided Porphinatoiron(II)s in Organic Solvents at 25 °C

	Solvent	$P_{1/2}{}^{O_2}$ / kPa	$10^{-7}\,k_{on}{}^{O_2}$ / $M^{-1}\,s^{-1}$	$10^{-3}\,k_{off}{}^{O_2}$ / s^{-1}	$10^{-6}\,k_{on}{}^{CO}$ / $M^{-1}\,s^{-1}$	$\tau_{1/2}{}^{O_2}$ / h
FeDP(H)	toluene	1.7[a)]	2.4[a)]	2.4[a)]	1.8[a)]	77
FeDP(OH)	CH_2Cl_2	33.5	0.0026	0.055	0.2	0.2
FeDP(OMe)	toluene	2.0	1.1	2.1	1.3	50
FeDP(OAc)	toluene	2.7	0.99	1.7	1.7	77
FeP	toluene	5.1[b)]	16[b)]	46[b)]	2.9[b)]	24

a) From Ref. 6. b) From Ref. 14.

ciation rate constants ($k_{on}^{O_2}$, $k_{off}^{O_2}$) were almost identical for **FeDP(H)**, **FeDP(OMe)**, and **FeDP(OAc)**, indicating that the nonprotic substituents on the 2,2-dimethylpropanoyloxy-fence groups did not cause any change in their O_2-binding equilibria and kinetics (Table 1). In contrast, **FeDP(OH)** showed an extremely low binding affinity for O_2 ($P_{1/2}^{O_2}$: 33.5 kPa), as opposed to the prediction that the H-bond would increase the O_2-binding affinity.[1,12,13] This is consistent with Kyuno's results.[10] In our case, the hydroxy groups form interfence H-bondings with the nearest carbonyls in the deoxy state; therefore, the extra binding energy of the O_2 molecule by the H-bond formation was cancelled out by cleavage of the former one. Our laser-flash experiments for **FeDP(OH)** revealed that the low O_2-binding affinity is kinetically ascribed to the small association rate constant by the steric hindrance, rather than by the decreased $k_{off}^{O_2}$ due to the H-bonding. The space-filling model showed that the four hydroxy end groups form H-bondings with the nearest neighboring esters,[19] so that each substituent could be noncovalently linked to construct a narrow pocket around the O_2-binding site. Indeed, the stretching frequency of the ester fences ($\nu_{C=O}$) of **FeDP(OH)** are shifted to the low frequency region relative to that of **FeDP(H)** ($1760 \rightarrow 1753\,cm^{-1}$), suggesting the H-bond formation. Moreover, the coordination of the hydroxy group to the central iron may also retard the O_2 association. These results showed that covalently attaching the nonprotic polar (methoxy or acetoxy) substituents on the 2,2-dimethylpropanoyloxy groups of the double-sided porphine does not change its O_2-binding parameter and the half-life of the dioxygenated complex in water-saturated toluene. On the other hand, the hydroxy groups significantly promote the irreversible oxidation and decrease the O_2-binding affinity, which is kinetically ascribed to the $1/10^3$-fold lower association rate constant compared to **FeDP(H)**.

FeDPs Incorporations into HSA. Serum albumin is the major transport protein, which binds a great variety of metabolites and organic compounds in our blood stream.[20,21] Despite the tremendous research on ligand bindings, there are only a few reports on the crystal structure of human serum albumin (HSA). The 585 amino acids consist of a unique heart-shaped structure, that is made of three repeating domains I to Ⅲ, and each one is constructed of two sub-domains.[22,23] The majority of the ligands is bound at one or both sites within special hydrophobic cavities of the subdomains ⅡA and ⅢA. A maximum of eight **FeP** molecules were incorporated into certain domains of human serum albumin with binding constants from 10^6–$10^4\ M^{-1}$.[7b,c] FeDPs were also expected to bind to HSA in a similar fashion, and the binding sites would also be identical. From quantitative analyses of the absorption intensity for the Soret band of aqueous **HSA–FeDP(OMe)**, the maximum binding numbers of **FeDP(OMe)** to an HSA were determined to be eight. The other FeDPs [**FeDP(H)**, **FeDP(OAc)**] also showed the same results. The binding numbers are always eight and independent of the polar substituents. The red-colored solution of HSA–FeDPs could be stored without any aggregation and precipitation for more than six months at 4 °C. The isoelectric points (pI) of the HSA–FeDPs [FeDPs/HSA = 8 (mol/mol)] were all 4.8 for **FeDP(H)**, **FeDP(OMe)** and **FeDP(OAc)** which was exactly the same as that of HSA. Fatty acid binding, for example, induced a reduction of the pI value due to partial neutralization of the surface charge. The FeDPs without any ionic residue interacts nonspecifically with a hydrophobic cavity of HSA. We concluded that the hydrophobic interaction is the major molecular force of the FeDP binding to HSA, and its incorporation does not induce any changes in the surface charge distribution of the host albumin.

O_2-Coordination Properties of HSA-FeDPs. The UV-vis absorption spectrum of the aqueous HSA including carbonyl **FeDP(OMe)** showed the formation of the typical CO-coordinated low-spin tetraphenylporphinatoiron(II) derivative (λ_{max}: 427, 546 nm) (Fig. 3). Light irradiation with a 500 W incandescent lamp of this solution under flowing O_2 led to CO dissociation, producing the dioxygenated species (λ_{max}: 426, 549 nm). Upon exposure of the dioxygenated HSA–**FeDP(OMe)** to N_2, the UV-vis absorption spectrum changed to that of a five-*N*-coordinated Fe^{2+} complex with an intramolecularly coordinated axial imidazole (λ_{max}: 438, 540, 560 nm). This dioxygenation was reversible and kinetically stable under physiological conditions (pH 7.3, 37 °C). The same O_2-adduct formation was also observed for the HSA hybrids with **FeDP(H)** and **FeDP(OAc)**.

However, the autooxidation reaction of the oxy state slowly occurred, and the absorption band of 549 nm almost disappeared after one day at 37 °C, leading to the formation of the inactive Fe^{3+} porphinate. The half-life of the dioxygenated species ($\tau_{1/2}$) of HSA–**FeDP(H)** was 5 h at 37 °C (pH 7.3, under 1 atm O_2), which is 2.5-fold longer compared to the $\tau_{1/2}$ of HSA–**FeP**.[7c]

The association and dissociation rate constants (k_{on}, k_{off}) of O_2 and CO were again explored by laser flash photolysis. The absorption decays that accompanied these gaseous recombinations were composed of three-phases of the first-order kinetics (Fig. 4), therefore the curves were fit by a triple-exponential equation, which is similar to the previously reported HSA–**FeP**.[7d] The minor, less than 10%, component, which has the fastest rate constant, was independent of the O_2 and CO con-

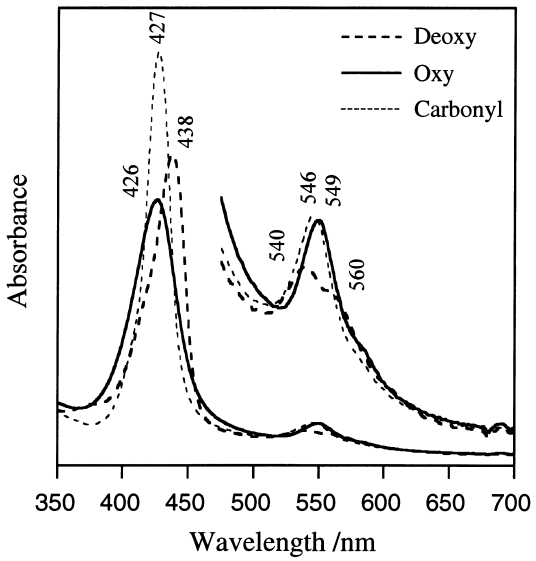

Fig. 3. Visible absorption spectral changes of HSA–**FeDP(OMe)** in phosphate buffer solution (pH 7.3) at 25 °C.

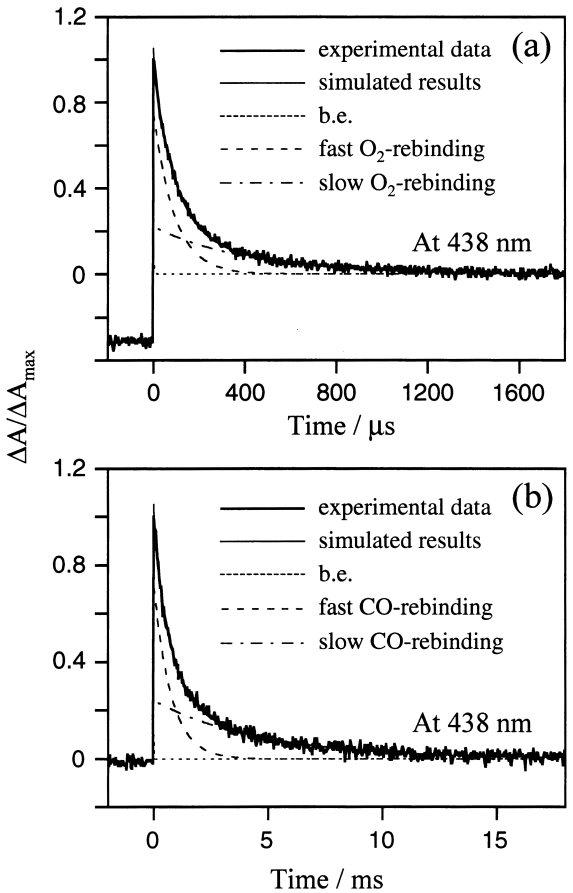

Fig. 4. Absorption decay of O_2 and CO rebinding to HSA–**FeDP(H)** in phosphate buffer solution after the laser flash photolysis at 25 °C. The kinetics was composed of total three phases and the relaxation curve can be well fitted by triple-exponentials. The component of b.e. is related to the base elimination. (a) The relaxation observed within ca. 1000 μs corresponds to the O_2-association to the five-coordinated **FeDP(H)**, and the much slower decay is reorganization from the O_2 complex to carbonyl complex. [O_2]: 81.7 kPa and [CO]: 9.2 kPa. (b) The relaxation decay observed within ca. 10 ms corresponds to the CO-association to five-coordinated **FeDP(H)**. [CO]: 101 kPa.

centrations. It is presumably correlated with a base elimination reaction.[22] Based on an evaluation of the other two phases, the association rate constants for the fast and slow rebindings (k_{on}(fast) and k_{on}(slow)) of O_2 and CO were calculated (Table 2). The $k_{on}^{O_2}$(fast) values are 4–7-fold greater than $k_{on}^{O_2}$(slow), and k_{on}^{CO}(fast) are 6–8-fold increase than k_{on}^{CO} (slow). The concentration ratio of the fast and slow reactions was approximately 3 for all the HSA–FeDPs [**FeDP(H)**, **FeDP(OMe)**, and **FeDP(OAc)**]. Therefore, we concluded that the O_2 association to FeDPs incorporated into the certain domains of serum albumin is mostly influenced by the molecular microenvironments around each O_2-coordination site, e.g. the steric hindrance of the amino acid residue and the difference in polarity. This completely fits the previous observation for HSA–**FeP**.[7d]

The $P_{1/2}^{O_2}$ of the HSA–FeDPs were determined on the basis of the UV-vis spectral changes during O_2 titration (Table 2). According to the results of kinetics experiments, the $P_{1/2}$ values were divided into two components using the previously reported equation.[7d] As expected, the isolated FeDP in HSA did not show a cooperative O_2-binding profile like that seen in Hbs; the Hill coefficient was 1.0. The $P_{1/2}^{O_2}$ value of HSA–**FeDP(H)**, for example, showed a relatively low value (3.1 kPa) compared to those of HSA–**FeP**, the red cells ($P_{1/2}^{O_2}$: 1.2 kPa), and **FeDP(H)** itself in the bilayer membrane of phospholipid vesicles (1.3 kPa).[6] It is noteworthy that the O_2- and CO-binding parameters are very similar for **FeDP(H)**, **FeDP(OMe)**, and **FeDP(OAc)**, indicating that the polar substituents on the fence groups did not cause any change in their equilibria and kinetics, even in albumin. Although the O_2-binding affinity of HSA–FeDPs are slightly low, the O_2-transporting efficacy in vivo between the lungs (P_{O_2}: 14.7 kPa) and muscle tissue (P_{O_2}: 5.3 kPa) is estimated to be ca. 20%, which is nearly the same value as that of the red cells.

Degradation of FeDPs in HSA by H_2O_2. H_2O_2 is a reactive oxygen species involved in the propagation of cellular injury during various pathophysiological conditions. It is known that the formation of H_2O_2 in red blood cells is associated with the autooxidation of oxy Hb.[24] Because most of the H_2O_2 is eliminated by catalase and glutathione peroxidase, the concentration of H_2O_2 in normal plasma is 4–5 μM (1 M = 1 mol dm^{-3}), but increases under inflammatory conditions.[25,26] In the presence of a small amount of H_2O_2 of 0.2 mM, the dioxygenated HSA–**FeDP(H)** rapidly oxidized within 30 min at 37 °C. Interestingly, following the oxidation of the Fe^{2+} ion, a very slow bleaching of the porphinate absorption was observed (Fig. 5). The solution became almost colorless after 5 days; the half-life ($\tau_{1/2}$) of this degradation was ca. 17 h. The more remarkable observation is that HSA–**FeP** bleached much faster than HSA–**FeDP(H)** with a $\tau_{1/2}$ of 0.5 h under the same condi-

Table 2. O_2- and CO-Binding Parameters of HSA Incorporating Double-Sided Porphinatoiron(II)s (FeDP/HSA = 8 (mol/mol)) in Phosphate Buffer Solution (pH 7.3, 25 °C)

	$P_{1/2}^{O_2}$/kPa		$10^{-7}\ k_{on}^{O_2}/M^{-1}\ s^{-1}$		$10^{-2}\ k_{off}^{O_2}/s^{-1}$		$10^{-6}\ k_{on}^{CO}/M^{-1}\ s^{-1}$		$\tau_{1/2}^{O_2}$/h
	fast	slow	fast	slow	fast	slow	fast	slow	(at 37 °C)
FeDP(H)	3.7	3.7	1.1	0.15	5.0	0.69	1.4	0.22	5
FeDP(OMe)	3.1	3.1	1.1	0.20	4.1	0.76	1.7	0.27	2
FeDP(OAc)	3.1	3.1	0.89	0.23	3.4	0.88	2.0	0.24	2
FeP[a)]	1.7	1.9	3.4	0.95	7.5	2.0	4.9	0.67	2

a) From Ref. 7d.

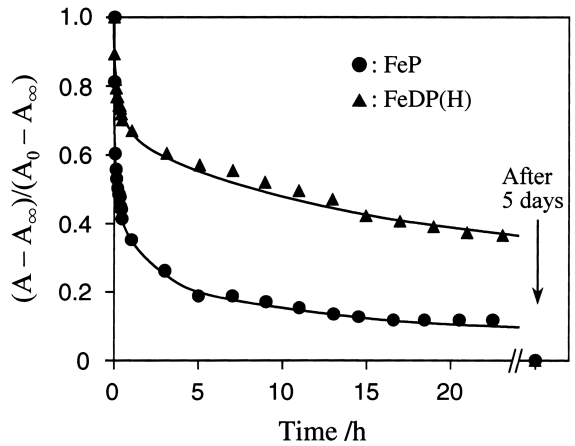

Fig. 5. Absorption decays of the Soret bands of HSA–**FeP** and HSA–**FeDP(H)** ([Fe]: 20 μM) in phosphate buffer solution (pH 7.3, 37 °C, under Air) in the presence of H_2O_2 of 0.2 mM.

tions. This difference clearly showed that the double-sided porphinatoiron has a high stability against H_2O_2. A detailed analysis of the products in these reactions is now underway.

In conclusion, human serum albumin incorporating double-sided porphinatoiron(II) derivatives as O_2-binding sites provides a synthetic O_2-carrying hemoprotein with a relatively long lifetime for the dioxygenated complexes under physiological conditions. The FeDPs binding to HSA is a hydrophobic interaction, which did not lead to a change in the surface charge of the HSA molecule. All eight FeDP complexes, in which the imidazolyl group is intramolecularly coordinated to the central Fe^{2+}, form reversible O_2 adducts in the albumin. The half-life of HSA–**FeDP(H)** became 5 h at 37 °C, which is 2.5-fold longer compared to that of HSA–**FeP**. Furthermore, **FeDP(H)** incorporated into the HSA structure showed a high stability against H_2O_2. The HSA incorporated double-sided porphinatoiron series may be useful for the synthetic analogue of the oxidation enzyme.

This work was partially supported by the Core Research for Evolutional Science and Technology, JST, Health Science Research Grants (Artificial Blood Project) of the Ministry of Health and Welfare, Japan, and a Grant-in-Aid for Scientific Research (No. 11650935) form the Ministry of Education, Science, Sports and Culture.

References

1 M. Momenteau and C. A. Reed, *Chem. Rev.*, **191**, 95 (1994), and references therein.

2 F. Tani, S. Nakayama, M. Ichimura, N. Nakamura, and Y. Naruta, *Chem. Lett.*, **1999**, 729.

3 a) P. Bhyrappa, J. K. Young, J. S. Moore, and K. S. Suslick, *J. Am. Chem. Soc.*, **118**, 5708 (1996). b) P. Bhyrappa, G. Vajiayanthimala, and K. S. Suslick, *J. Am. Chem. Soc.*, **121**, 263 (1999).

4 a) J. P. Collman, X. Zhang, V. J. Lee, and J. I Brauman, *J. Chem. Soc., Chem. Commun.*, **1992**, 1647. b) J. P. Collman, Z. Wang, A. Straumanis, and M. Quelquejeu, *J. Am. Chem. Soc.*, **121**, 460 (1999).

5 a) J. T. Groves, R. Neumann, *J. Am. Chem. Soc.*, **111**, 2900 (1989). b) J. Lahiri, G. D. Fate, S. B. Unsashe, and J. T. Groves, *J. Am. Chem. Soc.*, **118**, 2347 (1996).

6 E. Tsuchida, T. Komatsu, K. Arai, and H. Nishide, *J. Chem. Soc., Dalton Trans.*, **1993**, 2465.

7 a) T. Komatsu, K. Ando, N. Kawai, H. Nishide, and E. Tsuchida, *Chem. Lett.*, **1995**, 813. b) T. Komatsu, K. Hamamatsu, J. Wu, and E. Tsuchida, *Bioconjugate Chem.*, **10**, 82 (1999). c) E. Tsuchida, T. Komatsu, Y. Matsukawa, K. Hamamatsu, and J. Wu, *Bioconjugate Chem.*, **10**, 797 (1999). d) T. Komatsu, Y. Matsukawa, and E. Tsuchida, *Bioconjugate Chem.*, **11**, 772 (2000).

8 E. Tsuchida, T. Komatsu, K. Hamamatsu, Y. Matsukawa, A. Tajima, A. Yoshizu, Y. Izumi, and K. Kobayashi, *Bioconjugate Chem.*, **11**, 46 (2000).

9 C. K. Chang, B. Ward, R. Young, and M. P. Kondylis, *J. Macromol. Sci.-Chem.*, **A25**, 1307 (1985).

10 a) H. Imai, A. Nakatsubo, S. Nakagawa, Y. Uemori, and E. Kyuno, *Synth. React. Inorg. Met.-Org. Chem.*, **15**, 265 (1985). b) H. Imai, S. Sekizawa, and E. Kyuno, *Inorg. Chim. Acta.*, **125**, 151 (1986).

11 T. Komatsu, S. Kumamoto, H. Nishide, and E. Tsuchida, *Bull. Chem. Soc. Jpn.*, **66**, 1640 (1993).

12 G. E. Wuenschell, C. Tetreau, D. Lavalette, and C. A. Reed, *J. Am. Chem. Soc.*, **114**, 3346 (1992).

13 C. K. Chang, Y. Ling, and G. Avilés, *J. Am. Chem. Soc.*, **117**, 4191 (1995).

14 E. Tsuchida, T. Komatsu, S. Kumamoto, K. Ando, and H. Nishide, *J. Chem. Soc., Perkin Trans. 2*, **1995**, 747.

15 A. Nakagawa, T. Komatsu, and E. Tsuchida, *Bioconjugate Chem.*, **12**, (2001) in press.

16 J. P. Collman, J. I. Brauman, B. L. Iverson, J. L. Sessler, R. M. Morris, and Q. H. Gibson, *J. Am. Chem. Soc.*, **105**, 3052 (1983).

17 T. G. Traylor, S. Tsuchiya, D. Campbell, M. Mitchell, D. Stynes, and N. Koga, *J. Am. Chem. Soc.*, **107**, 604 (1985).

18 J. P. Collman, J. I. Brauman, K. M. Doxsee, T. R. Halbert, E. Bunnenberg, R. E. Linder, G. N. LaMar, J. D. Guadio, G. Lang, and K. Spartalian, *J. Am. Chem. Soc.*, **102**, 4182 (1980).

19 The optimum structures of the double-sided porphinatoirons were predicted by the ESFF forcefield simulation using an Insight II system (Molecular Simulations Inc.) on a Silicon Graphics O_2 computer. The structure was generated by alternative minimizations and annealing dynamic calculations from 1000 to 100 K.

20 U. Kragh-Hansen, *Pharmacol. Rev.*, **33**, 17 (1981), and references therein.

21 T. Peters Jr., *Adv. Protein Chem.*, **37**, 161 (1985). T. Peters Jr., "All about Albumin, Biochemistry, Genetics, and Medical Applications," Academic Press, San Diego (1997).

22 S. Curry, H. Mandelkow, P. Brick, and N. Franks, *Nat. Struct. Biol.*, **5**, 827 (1998).

23 J. Geibel, J. Cannon, D. Campbell, and T. G. Traylor, *J. Am. Chem. Soc.*, **100**, 3575 (1978).

24 H. P. Mirsa and I. Fridovich, *J. Biol. Chem.*, **247**, 6960 (1972).

25 Y. Yamamoto, M. H. Brodsky, J. C. Baker, B. M. Ames, *Anal. Biochem.*, **160**, 7 (1987).

26 P. C. Bragt and I. L. Bonta, *Agents Accounts*, **10**, 536 (1980).